Wilson C, Cloy J, Graham M & Hamlet L (2013) A microanalytical study of iron, aluminium and organic matter relationships in soils with contrasting hydrological regimes, *Geoderma*, 202-203, pp. 71-81.

This is the peer reviewed version of this article

A microanalytical study of iron, aluminium and organic matter relationships in soils with contrasting hydrological regimes.

Wilson, C.A.[1*], Cloy, J.M.[2], Graham, M.C.[2], Hamlet, L.[1]

1. Biological and Environmental Sciences, School of Natural Sciences, University of Stirling, Stirling, FK9 4LA.
2. School of Geosciences, Crew Building, the King's Buildings, West Mains Road, Edinburgh EH9 3JN.

* Corresponding author, c.a.wilson@stir.ac.uk +44 (0)1786 467817.

Abstract

It is recognised that interactions between mineral oxides and soil organic matter (SOM) are an important factor in the stabilisation of soil organic carbon (SOC). The nature of these interactions is particularly complex in gleyed soils that experience periodic waterlogging and changeable redox conditions. This study explores the complex patterns of iron (Fe) (hydr)oxides and SOM in three soils with contrasting hydrological regimes (Gleysol, Stagnosol and Cambisol). Micromorphological examination of undisturbed soil thin sections was teamed with SEM-EDS analysis and sequential dissolution of Fe pedofeatures to gain a better understanding of the mechanisms involved in SOM stabilisation by mineral oxides. All soils contained a diverse range of particulate SOM forms and Fe pedofeatures; the degree of impregnation of the Fe pedofeatures was found to increase with depth and a strong correlation between the presence of SOM and Fe pedofeatures was found to exist through all soils. Weakly crystalline Fe (hydr)oxides were found in association with partially degraded tissue residues and amorphous fine organic matter (OM). Strongly crystalline Fe (hydr)oxides were found in all impregnative Fe pedofeatures and high Fe/C ratios suggested precipitative processes rather than sorption dominate SOC sequestration in these features. In addition, at the core of some strongly impregnated Fe nodules, occluded well preserved organic tissues were identified. The study highlights the range of processes and complexity involved in SOC sequestration over mm to cm scales and untangling this complexity is vital to understanding and modelling terrestrial C fluxes. Whilst the methods used here are not without their complications, the value of micro-scale studies of undisturbed soil thin sections is clearly demonstrated.

Highlights:

- Soils of contrasting hydrological regimes had similar Fe (hydr)oxide/SOM interactions
- Weakly crystalline Fe (hydr)oxides had sorptive association with amorphous fine OM/tissue residues
- Strongly crystalline Fe (hydr)oxide had precipitative association with SOM
- Strongly crystalline Fe (hydr)oxide nodules encapsulate tissue residues

1. Background

Gleyed (waterlogged) soils are characterised by highly localised patterns of iron (Fe) (hydr)oxide concentration and depletion resulting from complex soil redox conditions. The spatial and temporal distribution of oxidising and reducing conditions in gleyed soils has been linked to groundwater and soil water chemistry, microbial activity, organic matter (OM) distribution, aggregation and void patterns (Lovely, 1991; Ottow, 1970). In a gleyed soil alternating reducing and oxidising conditions can be an important driver of the C cycle (Li et al., 2012); the microbially mediated reduction and oxidation of Fe (hydr)oxides can lead not only to the stabilisation of carbon but also to its release as dissolved organic carbon (DOC) (Stemmler and Berthelin, 2003), CO_2 and CH_4 (Zerva and Mencuccini, 2005).

Redoximorphic characteristics can be found in both Gleysol and Stagnosol soil types (FAO, 2006). The two soils are differentiated by their hydromorphic characteristics with Gleysols subject to subsoil saturation by groundwater, whilst Stagnosols form in response to impeded drainage resulting in saturation of the surface horizons (FAO, 2006). Gley soils are typically heterogeneous over scales of a few μm to a few mm, reflecting their complex structure and internal organisation. Thus, gley soils require *in-situ* analysis at the micro-scale to fully

understand the processes involved (Curmi et al., 1994). Traditional bulk, wet chemical analyses can lose this microscale information, limiting the quality of information recovered.

Total Fe (hydr)oxide content has been shown to correlate strongly with oxidation resistant SOC, suggesting Fe(hydr)oxides play a role in stabilising SOM (Eusterhouse et al., 2005a; Eusterhouse et al., 2005b; Wagai and Mayer, 2007; Wiseman and Püttmann, 2005). However, identification of the exact mechanism of SOM stabilisation has been more difficult (Kögel-Knabner et al., 2006). This may be due to multiple stabilisation mechanisms operating, with the nature of the interactions between SOM and Fe/Al (hydr)oxides determined by the chemical characteristics of the SOM and the types of mineral phases present. In studies of free draining Cambisols poorly crystalline Fe and Al (hydr)oxides have been shown to be more important than strongly crystalline mineral (hydr)oxides for the stabilisation of SOM (Spielvogel et al. 2008). Similarly Torn et al. (1997) identified a correlation between long-term trends in increased Fe (hydr)oxide crystallinity and decreased SOC levels. Simple sorptive processes at the SOM surface are thought to be important (Kaiser et al., 2000). However, Wagai and Mayer (2007) found the maximum sorption ratio of Fe (hydr)oxides means simple sorption alone could not be responsible for stabilising the bulk of SOC, and Wagai et al. (2013) highlighted the importance of organo-mineral complexes rather than sorption. A host of other processes including the formation of ternary SOM – Fe-oxide – clay associations (Wagai and Mayer, 2007) and unidentified chemical bonds (Spielvogel et al., 2008) have been suggested as possible mechanisms for stabilisation

Few studies have investigated the chemical composition of the SOM stabilised by Fe/Al (hydr)oxides in gleyed soils (Kaiser et al., 2000; Spielvogel et al., 2008), likewise the complex spatial pattern of oxidising and reducing conditions over very small scales has been given little consideration. Identifying the effects of any one of these processes in such spatially complex systems is difficult when using standard bulk wet chemical analyses, as the effects of multiple mechanisms may be being measured. Analysis of the distribution of SOM, Fe, Al, and other minerals (e.g. Si and Mn) in undisturbed gley soils over scales of microns to millimetres, carefully related to bulk soil chemistry could provide a means of studying the complex processes of SOC chemical stabilisation *in-situ.*

Micromorphological analysis of soil thin sections allows observation of the spatial relationships of Fe depletion and concentration features alongside organic matter and voids (Bouma et al., 1990; Curmi et al., 1994). Thin section micromorphology allows the

identification of redoximorphic properties not visible in the field or in bulk samples (Stolt et al., 2001). Selective dissolution of thin sections is a well-established technique in soil micromorphology (Bullock et al., 1985; Stoops, 2003), and when teamed with optical and chemical analysis of the slide or the solution can also be used to infer something about the nature of these components (Curmi et al., 1994). *In-situ* micro-chemical analysis of SOM and Fe pedofeatures has been successfully tried. For example, μ-XANES has been used to map Fe content, oxidation state and speciation in rock thin sections (Mũnoz et al., 2006), however, with this technique mapping is restricted to an area of less than 390 x 180 μm. Electron microprobe analysis allows chemical mapping of larger mm^2 areas and has been applied to chemical mapping of iron nodules (e.g. Dawson et al., 1985). Scanning Electron Microscopy – Energy Dispersive X-ray Spectrometry (SEM-EDS) has the advantage of being relatively cheap and rapid, thus allowing chemical mapping of larger areas (cm^2) through the montaging of smaller fields of view (e.g. Hapca et al., 2011), and when applied to soil thin sections the element distributions can be linked with features identified micromorphologically. As such it has been used to map element distributions in relation to Fe (hydr)oxides (Curmi et al., 1994) and soil structure (Smith, 2010), as well as heavy metal sorption sites in soils (Sipos et al., 2009). This comparative study of Stagnosols, Gleysols and Cambisols applied micromorphology, selective dissolution, and SEM-EDS in order to identify trends in the spatial patterns of SOM and Fe (hydr)oxides, and to determine the nature of the relationship between these soil components. The aim was to learn more about the nature of Fe-SOM relationships in gleyic soils and the implications of this for SOC dynamics in these soils. The specific objectives were:

1. Develop analytical protocols for the *in-situ* investigation of Fe-SOM interactions.
2. Characterise the relationship between Fe pedofeatures and SOM in gleyed soils with differing hydrological regimes.
3. Elucidate the nature of Fe-SOM interactions in gleyed soils through the application of *in-situ* analytical techniques.

2. Methods

2.1 Field Site and Sampling

The study site was Harwood Forest, Northumberland, UK (BNG NY 995 944; Figure 1). This commercially managed Sitka Spruce (*Picea sitchensis)* plantation dates back to the 1950s and was chosen because it is part of the CARBOEUROPE (www.carboeurope.org) and global FLUXNET (www.fluxnet.ornl.gov) projects. As such, the soils and carbon dynamics of the forest are already well documented (e.g. Zerva et al., 2005; Ball et al., 2007; Mojeremane et al., 2010). The forest covers an area of gentle slopes ($< 10^o$) at altitudes of between 200 and 400 m above ordnance datum (AOD). The underlying parent material is dominated by till and drift deposits derived from Paleozoic sandstones, mudstones and shales; these support Histosols, Gleysols, Stagnosols, Podzols and small areas of Cambisol soils (Avery, 1973; FAO, 2006). To avoid areas disturbed by deep ploughing and profile inversion, samples were taken from the non-forested grassy areas between plantation blocks, thus the sites were dominated by low-growing vegetation of grasses, mosses and herbs. Sample sites were identified based on detailed soil maps and an initial auger survey, and were chosen to cover a range of drainage and soil conditions. The chosen soils were histic Gleysol, histic Stagnosol, and gleyic Cambisol (FAO, 2006). These classifications were based on the local soil survey maps (Soil Survey of England and Wales, 1990) and local observation. The Gleysol soil profiles formed in sedimentary deposits on the margins of Fallowlees Loch, a small groundwater basin lake, and are affected seasonally by rises and falls in the groundwater levels. By contrast, the Stagnosol profiles were situated on a gentle ($5-10^o$) slope, and drainage in the upper part of the profile was restricted by the clay loam sub-soils derived from the local glacial drift geology. The Cambisol was located on an area of coarser textured sedimentary deposits alongside a small stream and although the deeper sub-soil exhibited some evidence of gleying the upper 45 cm was relatively free-draining.

At the Gleysol and Stagnosol sites, five 0.6 m x 0.6 m soil pits were opened to expose the soil profile, a further profile was opened in the Cambisol soil to act as a control (eleven soil pits in total). Undisturbed blocks of soil were cut from the face using Kubiena tins (8 cm high x 6 cm wide x 5 cm deep), three replicate samples were taken from within the 5-15 cm depth interval (or as appropriate to cover the organic and organo-mineral horizons) and a further sample was taken from the mineral sub-surface horizon between 20-30 cm (four Kubiena samples per soil pit, a total of 24 Kubiena samples in total). The Kubiena tins were sealed and refrigerated for transport back to the laboratory. In addition a monolith tin was used to recover the complete soil profile to a depth of 30 cm. This was sub-sampled at 10 cm

intervals for disturbed bulk soil samples. Typical soil profiles, described following Hodgson (1976) and Schoeneberger et al (2002), are provided in Table 1 for each of the soil types.

2.2 Analytical Methods

2.2.1 Thin section manufacture and analysis

Kubiena samples were freeze-dried in preference to traditional acetone drying to minimize the loss of acetone soluble materials. The dried samples were impregnated under vacuum with epoxy resin, and glass-mounted thin sections (ca. 40 µm thick) were manufactured according to standard methods (www.stir.ac.uk/thin; following Murphy, 1986). Thin sections were left uncoverslipped to allow SEM-EDS analysis and selective dissolution of the slide surface.

Thin sections were examined using an Olympus BX-50 petrological microscope at magnifications of between x 20 to x 200, and briefly described using standard micromorphological terminology (Bullock et al., 1985; Stoops, 2003; Stoops et al., 2010). The relative distribution and frequency of voids, SOM, and Fe pedofeatures were determined semi-quantitatively using point counting. Observations at x 100 magnification were made over a grid of 1.5 mm interval, giving a total number of 1250 - 1650 observation points per slide. At each observation point the feature(s) present was recorded according to one or more of the following classes: void (presence / absence), mineral (presence / absence), Fe pedofeature (depletion, weakly impregnated, moderately impregnated, strongly impregnated (orthic, anorthic or disorthic)) (Figure 2), and SOM (organ residue, tissue residue, cellular residue, amorphous fine organic material).

2.2.2 SEM-EDS analysis

SEM-EDS analysis (Zeiss EVO-MA15 with an Oxford Instruments InCA XMax 80 mm EDS) was used to determine the chemical composition of representative Fe pedofeatures and SOM features. Low vacuum conditions were used (60 Pa) to prevent surface charging without carbon coating the samples. Strict operating conditions of 50 µA filament current, 2.525 A gun current, 20 kV accelerating voltage, and 8.5 mm working distance to achieve an acquisition rate of 10 kcps were used to standardise the analyses, and a polished Co standard was analysed every 2 hours to adjust for beam current drift. The elemental results produced

by this method are semi-quantitative. Sites of interest were relocated between each stage of the dissolution procedure using stored images with three known reference points; this allowed a spatial accuracy of better than 10 μm. Given this 10 μm spatial discrepancy in relocating points and the small interaction volumes (2-3 μm radius) for each analysis, analyses were conducted across regions of interest 40 μm x 40 μm in size. In this way the potential influence of small <10 μm spatial discrepancies was minimised. At least three sites of interest were taken from each individual feature (as feature size allowed), and where possible a total of ten or more features were analysed, drawn from across both gley soil types. Sites of interest were located at least 50 μm from the edge of the SOM particles and Fe pedofeatures to limit edge effects and to avoid possible unidentified interferences or interactions with the encasing resin (Table 2). SEM-EDS analysis under these operating conditions allows simultaneous determination of all elements, heavier than beryllium, that are present in concentrations above the instrumental detection limits (0.5-0.8 % wt).

2.2.3 Selective dissolution

Following SEM-EDS analysis, a sequential extraction procedure applied to the surface of the thin sections resulted in the selective dissolution of Fe (hydr)oxides. The sequential procedure selected was chosen to mimic that applied to the analysis of bulk soil samples, some results from which are reported here (Table 3). The procedure used a two-step sequential extraction: step 1, immersion of the thin section in 0.02 M ammonium oxalate at pH 3 (Van Oorschot and Dekkers, 2001; Schwertmann, 1964) for 2 hours in dark room conditions on a shaking plate, and step 2, immersion of the thin section in a solution of citrate dithionite (10:1 0.3 M citrate and 1 M bicarbonate) at a sustained temperature of 70 ^{o}C for 15 minutes (Van Oorschot and Dekkers, 1999; Mehra and Jackson, 1960). Step one of the sequential extraction removes Al and Fe from weakly crystalline (hydr)oxides together with associated SOM, whilst step two removes Al and Fe from strongly crystalline (hydr)oxides together with associated SOM (Van Oorschot and Deckers, 2001). The 0.02 M ammonium oxalate extraction was used in preference to 0.2M ammonium oxalate, to minimise matrix contamination that interfered with FT-IR analysis of the extracts. Leaving thin sections in either the oxalate or citrate dithionite extraction solution for longer periods of time, resulted in no visible additional removal of material, but did weaken the bonding of the thin section to the glass slide resulting, in some cases, in the physical loss of material.

The Fe pedofeatures and SOM features analysed initially using SEM-EDS, were reanalysed following each step of the sequential extraction using the same techniques and identical operating conditions. Any interactions with the resin would be expected to be greatest at the particle edges where there is direct contact between the feature and resin. Preliminary tests of the selective dissolution procedure on strongly and moderately impregnated Fe nodules, demonstrated no visible or chemical differences in the response to the extractions in areas close to the edge (within 50 μm of the edge) as opposed to those within the interior (> 50 μm from the edge) (interaction effects, Table 2). The solutions used during the sequential selective dissolution were kept with the hope of recovering the extracted Fe and Al (hydr)oxides and SOM for FT-IR analysis. Unfortunately insufficient material was recovered by this process to allow direct analysis of the extracted material.

2.2.4 Bulk soil characterisation

The bulk soil properties were characterised using the monolith samples. Soil pH was determined using a 1:2 mixture of air-dried soil and deionised water. SOM content was determined by loss on ignition (LOI SOM) (16 hrs, $450^{o}C$), and particle size distribution was determined using a Coulter Counter LS230. Total Fe concentration was determined by ICP-OES (Perkin Elmer Optima 5300 DV) following microwave-assisted HNO_3/HBF_4 digestion. The accuracy of the total concentration data was monitored by the use of three certified reference materials; silty clay loam soil (CRM No. 7003), ombrotrophic peat (NIMT/UOE/FM001) and coal (NBS SRM 1635). Determined concentrations on average were 85-95 % (Fe) and 92-95 % (Al) of the certified values. Weakly crystalline Fe was extracted using 0.02M ammonium oxalate (pH 3) following van Oorschot & Dekkers (2001), and strongly crystalline Fe in a sequential extraction procedure using dithionite-citrate-bicarbonate (DCB) (Van Oorschot and Dekkers, 1999; Mehra and Jackson, 1960), Fe concentrations in the extract solution were determined by ICP-OES. C/N analysis of bulk soil and extracted residues was performed using a Carlo-Erba NA 1500 Elemental Analyser. Extracted residues were washed twice with deionised water and dried (30 °C; 48 hours) before analysis.

2.2.5 Data analysis

Data were sorted according to sampling depth, the soil horizon from which the observation was made and soil type. They were analysed using IBM SPSS ver. 19. Statistical analysis

involved the Anderson-Darling normality test, Chi Square analysis of the point count micromorphological data, and GLM ANOVA of SEM-EDS chemical and point counting frequency data, followed by Tukey pairwise comparisons. A significance level of $p \leq 0.05$ was used in all analyses.

3.   Results

The three soil types exhibited different field profiles (Table 1) reflecting their contrasting hydrological regimes. Both gley soils have a clearly defined organic (histic) horizon that is absent from the Cambisol. In the Gleysol, which is influenced by groundwater fluctuation, the surface organic horizon grades into an organo-mineral A horizon. In the Stagnosol, which is dominated by a perched watertable, the distinction between the organic and mineral horizons is sharper with the histic horizon giving way to a gleyed organo-mineral A(g) horizon. All three profiles exhibit evidence of gleyic processes in the form of Fe masses and nodules, but these are more frequent and more distinct in the gley soils than in the Cambisol. In the Stagnosol, redoximorphic features (masses and nodules) occur at a shallower depth (ca. 15 cm) than in either the Gleysol or Cambisol, reflecting the presence of restricted drainage in the upper soil horizons.

Physical and chemical characterisation of the soils showed all three soils to be predominately acidic (min pH 3.9, max pH 5.4), sandy loams (Table 3). The high LOI SOM content of the Ao horizons of the Gleysol and Stagnosol (24% in both) drops markedly into the A horizon and is similar to that of the Cambisol A horizon. LOI SOM concentrations remain over 4% to a depth of 30 cm + in all soils. Total Fe concentrations were found to be relatively static with depth in both the Cambisol and Stagnosol, whilst the Gleysol demonstrated a steady increase in total Fe with depth and the highest Fe concentrations overall. The Fe oxalate: Fe dithionite ratio shows relative changes in crystallinity of Fe (hydr)oxides with depth with the lowest values indicating higher crystallinity. In all three soils the ratio decreases with depth indicating an increased degree of crystallinity in the deeper soil horizons. The highest ratio, and hence lowest relative level of crystallinity (0.48), was found at 0-10 cm in the Gleysol. The amount of SOC associated with Fe (hydr)oxides in the bulk samples was highest in the 0-10 cm of the two gleyed soils, this decreased as expected with depth, although significant amounts of Fe (hydr)oxide associated SOC were found in the 20-30 cm horizons.

In thin section, all soils were found to contain a variety of SOM features and impregnative Fe pedofeatures (Figure 2). Fe pedofeatures ranged from weakly impregnated, irregularly shaped, orthic (internal groundmass consistent and continuous with that of the surrounding soil) impregnations (Figure 2-4) of the soil groundmass and SOM in the form of nodules and hypo-coatings, to strongly impregnated anorthic (internal groundmass consistent but not continuous with that of the surrounding soil) and / or disorthic (internal groundmass inconsistent with that of the surrounding soil) nodules (Figure 2-3 and 2-5), pans (Figure 2-1) and hypocoatings (Figure 2-6). These anorthic / disorthic nodules were massive in nature, showing no evidence of the internal concentric layering (e.g. Stiles et al. 2001) or more strongly impregnated rinds and internal zoning (Schulz et al. 2010) identified by other researchers.

Point counting focussed on the frequency and relative distributions of the soil features (Table 4). The results show that total % void space is highest in the Ao horizons, but due to the high level of variability no significant differences were found among soil types or horizons. However, as expected, mineral grain concentrations are significantly higher in the A and B horizons than in organic rich Ao horizons. The dominant class of SOM in all three soils, is amorphous organic fine material present either in discreet particles or mixed with fine mineral material forming the organo-mineral groundmass. Fresh, non-degraded organ residues (mainly root material, Figure 2-9) are relatively rare in all soils and soil horizons, but are most frequent in the Cambisol. Partially degraded tissue and cellular residues (Figure 2-8) are most frequent throughout the Stagnosol, particularly in the Ao horizon, but were rare in the Gleysol. Fe pedofeatures are common in all three soils including the Cambisol. Weakly impregnated orthic nodules are most frequent in the Gleysol and appear to be most common in the A horizon of both gleyed soils (Stagnosol A – 48.4%, Gleysol A(g) – 17.8%). The frequency of moderately impregnated orthic nodules decreases with depth in both the Gleysol and Stagnosol. Strongly impregnated anorthic and / or disorthic nodules were the least common class in the gleyed soils (Gleysol .7 – 1.4 %, Stagnosol 1.9 - 2.7 %), but are relatively common as rounded typic nodules in the Cambisol A horizon (6.1 %). Whilst no significant differences were found, there is a suggestion that these nodules increased in frequency with depth, particularly in the Gleysol soil.

In all three soils a significant positive correlation (χ) was found between the presence of SOM and the presence of Fe pedofeatures (Table 5). In the Cambisol, all SOM categories

were associated with orthic Fe pedofeatures. In the Stagnosol, orthic Fe pedofeatures are found in association with tissue and cell residues throughout the profile, whilst in the sub-soil amorphous organic fine materials are more commonly associated with anorthic or disorthic strongly impregnated Fe pedofeatures. In the Gleysol too, weakly and moderately impregnated orthic Fe pedofeatures are associated with cell and tissue residues throughout the soil profile, whilst the strongly impregnated anorthic and disorthic Fe pedofeatures are more strongly associated with amorphous fine organic material. Overall, however, there were no significant differences in SOM / Fe pedofeature associations between the Stagnosol and Gleysol profiles.

SEM-EDS analysis (Table 6) of the resin used to impregnate the sample reveals a high carbon content of 78 wt %, and negligible Fe and Al (0.32 wt %, 0.28 wt %). The mean O / C ratio of the crystic resin was 0.24 (SD 0.04). No significant differences were found between the chemistry of the two gley soil types, and hence they have been grouped together for subsequent analysis of individual SOM and Fe pedofeatures. The chemistry of the organo-mineral groundmass of the two gley soil types had a combined mean C content of 56 wt % and an O:C ratio of 0.58 in the 5-15 cm A horizons, and 36 wt % C with an O / C ratio of 1.15 in the subsoil. The Fe and Al contents of the gley soil groundmass are significantly higher than the resin at 0.74 wt % and 3.7 wt %, respectively in the topsoil and 3.1 wt % and 4.9 wt %, respectively in the subsoil. The groundmass of the Cambisol A horizon by contrast contained an average 65 wt % C (O / C 0.38) in the topsoil, and 1.4 wt % Fe and 1.7 wt % Al.

Organ and tissue residues show no significant difference in composition amongst all three soil types, with mean C concentrations of 67.9 wt %, an O / C ratio of 0.39, and variable trace concentrations of Si, Al, Fe, Ca, K, N, S and P. The average Fe / C and Fe & Al / C ratios of these fresh tissues are 0.03 and 0.04. Amorphous black fine organic material does not differ significantly in composition from the tissue residues with a mean C content of 71.4 wt %, and an O/C ratio of 0.35. Trace concentrations of Al (0.87 wt %), Fe (0.88 wt %), Si, Ca, K, and S are also present, giving Fe / C and Fe & Al / C ratios of 0.01 and 0.02, respectively.

The composition of the Fe pedofeatures is generally more variable than that of the soil groundmass or SOM features (Table 6); differences between individual pedofeatures are greater than differences due to soil type or depth. As a result each class of Fe (hydr)oxide features is presented separately, but without subdivision according to soil type or sample

depth. In all cases, (hydr)oxides of Fe dominate rather than Al (maximum 6.4 wt %), or Mn (maximum 2.1 wt %).

Tissue Fe impregnations have mean Fe / C and Fe & Al / C ratios of 0.35 and 0.38, respectively and an average Fe concentration of 9.0 wt %, which is significantly higher (p < 0.000) than fresh non-impregnated tissue residues. The O / C ratios (mean 0.71) also differed significantly from that of fresh non-impregnated organic tissues.

Weak to moderate Fe impregnations of the groundmass in the gley soils have a mean O / C ratio of 0.81 with an average C content of 47 wt % and Fe concentrations averaging 6.9 wt %; significantly higher than that of the non-impregnated groundmass of either the topsoil or sub soil. Fe / C and Fe & Al / C ratios averaged 0.18 and 0.26, respectively. As with the non-impregnated groundmass the overall composition of this material is highly variable.

The composition of strongly impregnated anorthic and disorthic Fe nodules was also variable and shows no significant differences either between the two gley soils or with depth through the soil profile. These strongly impregnated pedofeatures have the highest Fe / C, Fe & Al / C, and O / C ratios (1.93, 2.09, 2.59) measured with an average C content of 22 wt % and Fe and Al concentrations of 28 wt % and 2.7 wt %, respectively.

Following selective dissolution procedures the resin loses a small but significant amount of C following each procedure (Table 6). The largest drop, from 78 wt % to 72 wt % C, occurs following the oxalate extraction, with a smaller decline to 69 wt % C following the dithionite stage. There is no significant effect on the Fe concentrations in the resin from the oxalate stage; however, there is a small but significant decline in Fe following the dithionite extraction. Resin Al concentrations appear to have been unaffected by either procedure.

There are no significant changes in C concentration in the fresh tissue residues, although they did experience significant drops in Al (0.75 wt % - 0.16 wt % Al) and Fe (1.98 wt % - 0.21 wt % Fe) concentrations following the oxalate extraction process. Black amorphous fine organic material also shows no loss of C, but significant decreases in Al (0.87 wt % - 0.33 wt % Al) following the oxalate extraction and in Fe following both the oxalate and dithionite extractions (0.88 wt % - 0.28 wt % - 0.04 wt % Fe).

There is no significant loss of C from the groundmass of the soils during the treatments. However, Fe concentrations do decline significantly in the topsoil of the Cambisol and the

subsoil of the Gleysol following the dithionite extraction. Fe concentrations in the Gleysol topsoil (5-15 cm) declined following both the oxalate and dithionite extraction steps (0.74 wt % - 0.30 wt % - 0.15 wt % Fe).

Fe pedofeatures have a different pattern of chemical change following the extraction procedure. Al concentrations show no significant change in concentration throughout the process. In the orthic groundmass impregnations, Fe concentrations decline significantly after each step (6.9 wt % - 2.5 wt % - 0.23 wt % Fe), whilst C concentrations increase by a similar amount. As a result Fe / C ratios decrease significantly through the process starting at 0.18 and decreasing to 0.05 following oxalate extraction and then to 0.01 after the dithionite step.

Tissue Fe impregnations also show a significant decline in Fe through the process (9.0 wt % - 5.0 wt % - 0.00 wt % Fe), with small, but not significant, increases in C concentration. The Fe / C ratio declines throughout the process, but the only significant change follows the dithionite stage (0.35 - 0.11 - 0.00). The effect of the dithionite step is graphically illustrated in Figure 3 in the Back Scattered Electron (BSE) image of an impregnated root tissue before and following each step. The oxalate extraction makes little visible impact on the feature, whilst dithionite removes Fe completely leaving the original root tissues exposed including preserved cellular tissues.

Strongly impregnated anorthic Fe nodules show a significant change in Fe / C ratio after each treatment with a trend towards decreased Fe relative to C. In this case Fe concentrations decrease significantly after each step, but the largest drop follows the final dithionite extraction (28 wt % - 23 wt % - 0.59 wt % Fe). C concentrations by contrast rise significantly (22 wt % - 29 wt % - 48 wt % C). These changes to the chemistry of the black anorthic Fe nodules are clearly exemplified by the BSE images (Figure 3), which show the complete loss of an encapsulating shell of Fe (hydr)oxides following the dithionite step to reveal a fragment of organic tissue residue with some cellular detail preserved.

4. Discussion

Micromorphological examination revealed a complex array of SOM and Fe impregnation pedofeatures. SOM ranged in form from fresh, identifiable organ residues (typically roots) to amorphous organic fine material and the homogenised organo-mineral groundmass of the

soil. In the Stagnosol, the distinct histic surface horizon resulted in higher proportions of identifiable tissue residues. Although the histic surface horizon was absent from the Cambisol, organ and tissue residues were frequent in the upper soil horizon because of the frequency of root features.

The dominance of Fe rather than Mn in Fe pedofeatures was confirmed by SEM-EDS analysis and suggests that saturation periods are often prolonged (> 2-3 days) in these soils (Veneman et al. 1976; Hseu and Chen, 1999; He et al. 2003; Kyuma, 2004; Zaidel'man et al., 2009). This interpretation is supported by the low chroma field colours (≤ 2) of the Gleysol and Stagnosol A horizons (Franzmeier et al. 1983; Vepraskas and Wilding, 1983), whilst the higher chroma (4) of the Cambisol A horizon suggests a more freely-drained, oxidised soil environment (Table 1) (Vepraskas, 1999). This supports the field observations concerning local hydrology and soil drainage that were made at the sites.

Weak and moderately impreganted orthic Fe nodules were the most common pedofeature in all soils, and in the gleyic soils they were particularly dominant in the upper soil horizons, whilst strongly impregnated nodules and hypocoatings were more common in the deeper subsoils. The A horizon of the Cambisol contained more strongly impregnated Fe pedofeatures than either of the gleyed soils. The smooth sharp edges of the strongly impregnated anorthic / disorthic nodules can form following a drop in ground water levels when percolating rainwater removes less resistant Fe (hydr)oxides from their edges (PiPujol and Buurman, 1994; Pipujol and Buurman, 1998). The higher relative incidence of anorthic / disorthic Fe nodules in the Cambisol supports the more freely drained hydrological regime of this soil, albeit with short, infrequent periods of waterlogging. The micromorphological (Table 4) evidence supports the taxonomic field classifications of Gleysol and Stagnosol. The results, however, fail to show any statistically significant differences between the Gleysol and Stagnosol with regard to the frequency, nature and distribution of Fe pedofeatures. This might suggest that either the two soils have similar hydrological regimes, a suggestion not supported by the topographic settings and morphology of the soils, or the hydrological differences were not great enough to differentially affect the development of redoximorphic conditions and the resulting micro-scale pattern of Fe (hydr)oxides. The distribution of Fe pedofeatures and SOM revealed a strong correlation between the presence of SOM and the presence of Fe pedofeatures in all three soil types indicating the importance of SOM in their formation.

The mean O / C ratio of the epoxy resin was 0.24, and significantly lower than the O / C ratios of tissue residues (0.39) and black amorphous fine organic material (0.35), which themselves are broadly within the accepted O/C range for lignin and soil humic acids (Malcolm and MacCarthy, 1986; Stoffyn-Egli et al., 1997). This accordance between published O/C values and the values determined in this study suggests that the background resin signal is small in these discreet features. However, the C concentrations recorded for the groundmass (between 36 and 65 wt % C) are clearly an overestimate, and although visible resin filled pores were avoided in the analysis, the effects of microporosity and resin entering the groundmass via capillary forces result in an unknown and variable contribution of C from the resin (Smith, 2010). Interpretation of SOM behaviour in the groundmass must therefore be treated cautiously. However, Fe concentrations in the resin were very low (0.32 wt % Fe) in relation to those of the groundmass (1.7 - 4.9 wt % Fe), and this correlates well with the bulk soil determinations of Fe of between 10-23 mg g^{-1} (Table 3).

As expected, the highest Fe/C ratios were in the strongly impregnated Fe nodules (1.93). Whilst SOM residues contained low concentrations of Fe, with Fe / C ratios of 0.01 – 0.03, weakly impregnated tissue residue showed a moderate, but significant enhancement in Fe (0.35 wt % Fe) as did the weakly impregnated groundmass (0.18 wt % Fe). Interestingly, the iron pan feature identified at the base of the A horizon in one of the Stagnosol profiles contained only a moderate concentration of Fe (4.9 wt % Fe, Fe / C ratio 0.08). This may suggest the presence of organically chelated Fe and Al, perhaps indicating formation of the iron pan through podzolisation rather than gleyic processes (Breunig-Madsen et al., 2000). However, the bulk chemical data (Table 3) does not show the marked down profile patterns in Fe and Al concentrations that would be expected from extensive podzolisation (Melkerud et al., 2000). As expected, Al makes a significant contribution to the Fe & Al / C ratios of the groundmass and groundmass impregnations due to the presence of clay minerals, but is only a minor component of the other Fe pedofeatures.

Whilst the visual impact of the oxalate extraction procedure on the thin sections was negligible, significant chemical changes were identified. The oxalate extraction resulted in a small loss of C from the resin, but the Fe / C ratio was unchanged allowing meaningful comparison between treatments. Organic tissue residues and black amorphous fine organic matter were also affected by the oxalate extraction process, with small but significant losses of Fe indicating the presence of weakly crystalline Fe (hydr)oxides. The importance of

weakly crystalline Fe (hydr)oxides for SOM stabilisation has been argued by Schnitzer and Kodama (1992) and Spielvogel et al. (2008), whilst Wiseman and Püttmann (2005) suggest sorptive processes are the dominant form of interaction between SOM and weakly crystalline Fe in Gleysols. The maximum sorptive capacity of Fe (hydr)oxides has been calculated as below 0.22 wt/wt (Wagai and Mayer, 2007); the ratios identified for SOM and the soil groundmass in this study are all well below this figure (0.01 - 0.09), and even allowing for the potential contamination by resin C, this suggests that sorption may be an important mechanism. The results of this study highlight the importance of weakly crystalline Fe (hydr)oxides in the stabilisation of amorphous fine organic matter fractions. Small but significant losses of Fe were also recorded from the weakly and strongly impregnated orthic Fe nodules, interestingly tissue impregnations did not appear to contain significant quantities of weakly crystalline Fe.

By contrast the dithionite extraction had more immediate and noticeable effects on the soil thin sections. The removal of strongly crystalline Fe (hydr)oxides, such as goethite, from the soils resulted in the almost complete removal of impregnative Fe pedofeatures from all three soils (Figure 3). The soil groundmass was not visibly affected and the C concentrations in the groundmass showed no significant change for any soil or soil horizon. However, the more freely-drained Cambisol topsoil did show a significant decrease in Fe following the removal of the strongly crystalline Fe (hydr)oxides. No significant effect was identified in the gley sub-soils suggesting that strongly crystalline Fe (hydr)oxides are a minor component of the groundmass of these soils, presumably as a result of Fe (hydr)oxide dissolution via reductive processes (e.g. Favre et al., 2002). The results indicate that strongly crystalline Fe (hydr)oxides dominate, even in weakly impregnated pedofeatures, however, it must be remembered that the 0.02M ammonium oxalate extractant used may not have fully recovered the weakly crystalline Fe (hydr)oxide fraction and their importance is thus being underestimated in this study. The Fe/C ratios of the impregnative Fe pedofeatures is high and suggests that precipitative processes involving organic chelates dominate rather than simple sorption (Wagai and Mayer, 2007), in line with prevailing theories as to their formation (e.g. Gasparatos et al., 2005).

This study also revealed weakly decomposed tissue residues encapsulated at the core of some of the strongly impregnated Fe (hydr)oxide nodules. As these residues were only revealed after dithionite dissolution of strongly crystalline Fe (hydr)oxides, and since their crystallinity

is known to increase over time via cycles of wetting and drying (Thompson et al., 2006), it can be assumed that these SOM fragments are relatively old. Further research is required to date these residues. The core of organic material in at least some of these strongly impregnated nodules appears to be of a lignified form due to the cells elongated form and thick walls (Stoops, 2003; Stolt and Linbo, 2010).

One possible mechanism for these nodules formation is by fungal-mediated oxidative degradation of lignin via phenol oxidase using ferrous iron (Fe^{2+}), from the wider soil environment, as a catalyst (Wood, 1994; Filley et al., 2002; Martínez et al., 2005; Van Bodeom et al., 2005), and resulting in the precipitation of ferric iron (Fe^{3+}). The spatially complex redox conditions present in gleyed soils, provides the mix of oxic and anoxic conditions necessary to drive this process. Schulz et al. (2010) has also proposed a fungal mediated precipitation mechanism for the formation of Fe (hydr)oxide nodules after identifying hyphae in their core, and the preferential reduction of amorphous to crystalline Fe by decomposing bacteria using Fe^{3+} as electron acceptors (Munch and Ottow, 1980) may also help to partially explain the high Fe (hydr)oxide crystallinity of the gleyed soils. Further analysis of extracted nodules from these soils to test for the presence of fungal hyphae, as well as to evaluate the role abiotic processes would be useful in resolving the exact mechanism involved.

The strongly impregnated Fe nodules were the least abundant class of Fe pedofeatures in all soils. However, in the gleyed soils their frequency increased with depth suggesting that such encapsulation within precipitated Fe (hydr)oxides could represent a small but significant stock of stabilised carbon in sub-soils. The stability of strongly crystalline Fe (hydr)oxides in predominantly aerobic soils means this mechanism may potentially provide long-term protection of SOM, and further research is needed to quantify this effect.

As suggested by Wagai and Mayer (2007) the SOM - mineral oxide relationships revealed in this study are not confined to simple surface sorption processes, but instead include a more diverse and complex array of interactions, such as precipitation of crystalline Fe (hydr)oxides and encapsulation of SOM. Surface adsorption has been demonstrated to be of importance in a range of soil types (Kaiser et al., 2000; Wagai et al., 2009) including soils affected by alternating reductive and oxidative conditions. This study supports the importance of adsorption mechanisms, identifying adsorption from the low Fe/C ratios and weakly crystalline nature of Fe (hydr)oxides associated with the gley soil groundmass and organ

residues. However, the role of more strongly crystalline Fe (hydr)oxides has also been highlighted with the high Fe/C ratios of strongly impregnated Fe nodules and tissue residues pointing towards the precipitation of chelates and the occlusion of tissue residues at the core of some strongly impregnated tissues.

Although further research is need to quantify the specific processes and investigate the role of abiotic factors, the approach used here has helped to demonstrate the nature and complexity of specific relationships between SOM and Fe and Al (hydr)oxides on the micro-scale. Spatial analysis of Fe pedofeatures in relation to void systems (perhaps employing μ X-CT) would allow investigation of abiotic factors. Further developments could include SEM mounted Raman and FT-IR analyses to provide a complementary method of analysing Fe-SOM interactions, whilst micro-XRD could help establish the mineralogical nature of the Fe (hydr)oxide features, but would require physical extraction of iron nodules from the thin section and glass slide mount (e.g. Arocena et al. 1994; Gasparatos et al., 2004) and thus could not be carried out in conjunction with the selective dissolution process. Whilst resin impregnation of the soil groundmass in thin sections is a limiting factor, the in-situ observations afforded are invaluable and coupled with micro-chemical analyses provide a powerful tool for the study of SOM – mineral interactions.

5.   Conclusion

This study has demonstrated that the *in-situ* analysis of undisturbed soils using optical microscopy, SEM-EDS and selective dissolution at structurally relevant micro-scales can yield important information about the complex nature of the processes involved in SOM sequestration. The results of this study have suggested that whilst weakly crystalline Fe (hydr)oxides and sorption mechanisms are important in the soil groundmass and partially degraded organic tissues, strongly crystalline Fe (hydr)oxide features appear to sequester OM in Fe-SOM complexes and via encapsulation at the core of Fe nodules. If we assume that different forms of SOM – Fe (hydr)oxides will react differently to environmental perturbations, this has implications for the long-term stability of sequestered SOC. Further application of *in-situ*, micro-scale analytical techniques to soils is needed to resolve this complexity.

6. Acknowledgements

7. References

Arocena, J.M., Pawluk, S., Dudas, M.J., 1994. Iron oxides in iron-rich nodules of sandy soils from Alberta (Canada), in: Ringrose-Voase, A.J., Humphreys, G.S., (Eds.), Soil micromorphology: studies in management and genesis. Proceedings of the IX International Working Meeting on Soil Micromorphology, Townsville, Australia, July 1992. Elsevier, Amsterdam, pp. 83-97.

Avery, B.W., 1973. Soil classification in the soil survey of England and Wales. Journal of Soil Science. 24, 324-338.

Ball, T., Smith, K.A., Moncrieff, J.B., 2007. Effect of stand age on greenhouse gas fluzes from a Sitka spruce [Picea sitchensis (Bong.) Carr.] chronosequence on a peaty gley soil. Global Change Biology. 13, 2128-2142.

Bouma, J., Fox, C.A., Miedema, R., 1990. Micromorphology of hydromorphic soils: applications for soil genesis and land evaluation, in: Douglas, L.A., (Ed.), Soil micromorphology: a basic and applied science. Proceedings of the VIIIth International Working Meeting of Soil Micromorphology, San Antonio, Texas, July 1988. Developments in Soil Science, 19, Elsevier, Amsterdam, pp. 257- 278.

Breunig-Madsen, H., Rønsbo, J., Holst, M.K., 2000. Comparison of the composition of iron pans in Danish burial mounds with bog iron and spodic material. Catena. 39, 1-9.

Bullock, P., Federoff, N., Jongerius, A., Stoops, G., Tursina, T., Babel, U., 1985. Handbook for soil thin section description. Waine Research Publications, Wolverhampton.

Curmi, P., Soulier, A., Trolard, F., 1994. Forms of iron oxides in acid hydromorphic soil environments: morphology and characterization by selective dissolution, in: Ringrose-Voase, A.J., Humphreys, G.S., (Eds.), Soil Micromorphology: studies in management and genesis. Developments in Soil Science, 22, Elsevier, Amsterdam, pp. 133-141.

Dawson, B.S.W., Fergusson, J.E., Campbell, A.S., Cutler, E.J.B., 1985. Distribution of elements in some Fe-Mn nodules and an iron-pan in some gley soils of New Zealand. Geoderma. 35, 127-143.

Eusterhues, K., Rumpel, C., Kögel-Knaber, I., 2005a. Stabilization of soil organic matter isolated via oxidative degradation. Organic Geochemistry. 36, 1567-1575.

Eusterhues, K., Rumpel, C., Kögel-Knaber, I., 2005b. Organo-mineral associations in sandy acid forest soils: importance of specific surface area, iron oxides and micropores. European Journal of Soil Science. 56, 753-763.

FAO, 2006. World reference base for soil resources 2006: a framework for international classification, correlation and communication. World Soil Resources Report, 103, FAO, Rome.

Favre, F., Tessier, D., Abdelmoula, M., Génin, J.M., Gates, W.P., Boivin, P., 2002. Iron reduction and changes in cation exchange capacity in intermittently waterlogged soil. European Journal of Soil Science. 53, 175-183.

Filley, T.R., Cody, G.D., Goodell, B., Jelllison, J., Noser, C., Ostrofsky, A., 2002. Lignin demethylation and polysaccharide decomposition in spruce sapwood degraded by brown rot fungi. Organic Geochemistry. 33, 111-124.

Franzmeier, D.P., Yahner, J.E., Steinhardt, G.C., Sinclair, H.R., 1983. Color patterns and water table levels in some Indiana soils. Soil Science Society of America Journal. 47, 1196-1202.

Gasparatos, D., Haidouti, C., Tarendis, D., 2004. Characterization of iron oxides in Fe-rich concretions from an imperfectly drained Greek soil: a study by selective dissolution techniques and X-ray diffraction. Archives of Agronomy and Soil Science. 50, 485-493.

Gasparatos, D., Tarenidis, D., Haidouti, C., Oikonomou, G., 2005. Microscopic structure of soil Fe-Mn nodules: environemntal implication. Environmental Chemistry Letters. 2, 175-178.

Hapca S.M., Wang, Z.X., Otten, W., Wilson, C., Baveye, P.C., 2011. Automated statistical method to align 2D chemical maps with 3D X-ray computed micro-tomographic images of soils. Geoderma. 164, 146-154.

He, X., Vepraskas, M.J., Lindbo, D.L., Skaggs, R.W., 2003. A method to predict soil saturation frequency and duration from soil color. Soil Science Society of America Journal. 57, 961-969.

Hseu, Z.Y., Chen, Z.S., 1999. Micromorphology of redoximorphic features of subtropical anthraquic Ultisols. Food Science and Agricultural Chemistry. 1, 194-202.

Hodgson, J.M., 1976. Soil survey field handbook. Soil Survey Technical Monograph No. 5, Soil Survey of England and Wales, Harpenden.

Kaiser, K., Haumaier, L., Zech, W., 2000. The sorption of organic matter in soils as affected by the nature of soil carbon. Soil Science. 165, 305-313.

Kögel-Knabner, I., Chenu, C., Kandeler, E., Piccolo, A., 2006. Biological and physicochemical processes and control of soil organic matter stabilization and turnover. European Journal of Soil Science. 57, 426–445.

Kyuma, K., 2004. Paddy Soil Science. Kyoto University Press and Trans Pacific Press. Melbourne.

Li, Y., Yu, S., Strong, J., Wang, H. (2012) Are the biogeochemical cycles of carbon, nitrogen, sulphur and phosphorus driven by the "Fe^{III}-Fe^{II} redox wheel" in dynamic redox environments? Journal of Soils and Sediments, 12, 683-693.

Lovley, D.R., 1991. Dissimilatory Fe(III) and Mn(IV) reduction. Microbiological Reviews. 55, 259-287.

Malcolm, R.L., MacCarthy, P., 1986. Limitations in the use of commercial humic acids in water and soil research. Environmental Science and Technology. 20, 904-911.

Martínez, Á.T., Speranza, M., Ruiz-Dueñas, F.J., Ferreira, P., Camarero, S., Guillén, F., Martínez, M.J., Gutiérrez, A., del Rio, J.C., 2005. Biodegradation of lignocellulosics: microbial, chemical and enzymatic aspects of the fungal attack of lignin. International Microbiology. 8, 195-204.

Mehra O.P., Jackson M.L., 1960, Iron oxide removal from soils and clays by dithionite-citrate systems buffered with sodium bicarbonate. Clays and Clay Minerals. 7, 317-327.

Melkerud, P.-A., Bain, D.C., Jongmans, A.G., Tarvainen, T., 2000, Chemical, mineralogical and morphological characterization of three podzols developed on glacial deposits in Northern Europe. Geoderma, 94, 125-148.

Mojeremane, W., Rees, R.M., Mencuccini, M., 2010. Effects of site preparation for afforestation on methane fluxes at Harwood Forest, NE England. Biogeochemistry. 97, 89-107.

Munch, J.-C, Ottow, J.C.G., 1980. Preferential reduction of amorphous to crystalline iron oxides by bacterial activity. Soil Science. 129, 15–21.

Mũnoz, M., De Andrade, V., Vidal, O., Lewin, E., Pascarelli, S., Susini, J., 2006. Redox and speciation micromapping using dispersive X-ray absorption spectroscopy: application to iron in chlorite mineral of metamorphoc rock thin section. Geochemistry, Geophysics, Geosystems. 7, Q11020, doi: 10.1029/2006GC001381.

Murphy, C.P., 1986. Thin section preparation of soils and sediments. AB Academic Publishers. Berkhamsted.

Ottow, J.C.G., 1970. Bacterial mechanism of gley formation. Nature. 225, 103.

PiPujol, M.D., Buurman, P., 1994. The distinction between ground-water gley and surface water gley phenomena in Tertiary paleosols of the Ebro Basin (NE Spain). Palaeogeography, Palaeoclimatology, Palaeoecology. 110, 103-113.

PiPujol, M.D., Buurman, P., 1998. Analyzing ground-water gley and surface-water (pseudogley) effects in paleosols. Quaternary International. 51-52, 77-79.

Schnitzer, M., Kodama, H., 1992. Interactions between organic and inorganic components in particle-size fractions separated from four soils. Soil Science Society of America Journal. 56, 1099-1105.

Schoeneberger, P.J., Wysocki, D.A., Benham, E.C., Broderson, W.D. (2002) Field book for describing and sampling soils, version 2.0. National Resources Conservation Service, Lincoln.

Schulz, M.S, Vivit, D., Schulz, C., Fitzpatrick, J., White, A., 2010. Biologic origin of iron-rich soil nodules in a marine terrace chronosequence, Santa Cruz, California. Soil Science Society of America Journal. 74, 550-564.

Schwertmann, U., 1964. Differenzierung der eisenoxide des bodens durch photochemische extraktion mit saurer ammoniumoxalate-lösung, Z. Pflanzenernährung, Düngung Bodenkunde. 105, 194-202.

Sipos, P., Németh, T., Kis, V.K., Mohai, I., 2009. Association of individual soil mineral constituents and heavy metals as studied by sorption experiements and analytical electron microscopy analyses. Journal of Hazardous Materials. 168, 1512-1520.

Smith, K.E., 2010. The nature, distribution and significance of organic carbon within structurally intact soils contrasting in total SOC content. Unpublished PhD thesis, University of Stirling, Stirling

Soil Survey of England and Wales (1990) Soils of the Alnwick and Rothbury District, 1:50000 coloured soil map. Soil Survey of England and Wales, Rothamsted.

Spielvogel, S., Prietzel, J., Kögel-Knaber, I., 2008. Soil organic matter stabilization in acidic forest soils is preferential and soil-type specific. European Journal of Soil Science. 59, 674-692.

Stemmler, S.J., Berthelin, J., 2003. Microbial activity as a major factor in the mobilization of iron in the humid tropics. European Journal of Soil Science. 54, 725-733.

Stiles, C.A., Mora, C.I., Driese, S.G., 2001. Pedogenic iron-maganese nodules in Vertisols: a new proxy for palaeoprecipitation. Geology. 29, 943-946.

Stoffyn-Egli, P., Potter, T.M., Leonard, J.D., Pocklington, R., 1997. The identification of black carbon particles with the analytical scanning microscope:methods and initial results. Science of the Total Environment. 198, 211-223.

Stolt, M.H., Lesinski, B.C., Wright, W., 2001. Micromorphology of seasonally saturated soils in carboniferous glacial till. Soil Science. 166, 406-414.

Stolt, M.H., Linbo, D.L., 2010. Soil organic matter, in: Stoops, G., Marcelino, V., Mees, F., (Eds.), Interpretation of micromorphological features of soils and regoliths. Elsevier Science Ltd, Amsterdam, pp. 369-395.

Stoops, G., 2003. Guidelines for analysis and description of soil and regolith thin sections. Soil Science Society of America, Madison.

Stoops, G., Marcelino, V., Mees, F., 2010. Interpretation of micromorphological features of soils and regoliths. Elsevier Science Ltd, Amsterdam.

Thompson, A., Chadwick, O.A., Rancourt, D.G., Chorover, J., 2006. Iron-oxide crystallinity increases during soil redox oscillations. Geochimica et Cosmochimica Acta. 70, 1710-1727.

Torn, M.S., Trumbore, S.E., Chadwick, O.A., Vitousek, P.M., Hendricks, D.M., 1997. Mineral control of soil organic carbon storage and turnover. Nature. 389, 170-173.

Van Bodeom, P.M., Broekman, R., Van Dijk, J., Bakker, C., Aerts, R., 2005. Ferrous iron stimulates phenol oxidase activity and organic matter decomposition in waterlogged wetlands. Biogeochemistry. 76, 69-83.

Van Oorschot I.H.M., Dekkers M.J., 1999. Dissolution behaviour of fine-grained magnetite and maghemite in the citrate-bicarbonate-dithionite extraction method. Earth and Planetary Science Letters. 167, 283-295.

Van Oorschot I.H.M., Dekkers M.J., 2001. Selective dissolution of magnetic iron oxides in the acid-ammonium oxalate/ferrous iron extraction method – I. Synthetic samples. Geophysical Journal International. 145, 740-748.

Veneman, P.L.M., Vepraskas, M.J., Bouma, J., 1976. The physical significance of soil mottling in a Wisconsin toposequence. Geoderma. 15, 103-118.

Vepraskas, M.J., 1999. Redoximorphic features for identifying aquic conditions. Technical Bulletin 31, North Carolina Agricultural Research Sevice, Raleigh, North Carolina.

Vepraskas, M.J., Wilding, L.P., 1983. Aquic moisture regimes in soils with and without low chroma colours. Soil Science Society of America Journal. 47, 280-285.

Wagai, R., Mayer, L.M., 2007. Sorptive stabilization of organic matter in soils by hydrous iron oxides. Geochimica et Cosmochimica Acta. 71, 25-35.

Wagai, R., Mayer, L.M., Kitayama, K., 2009. Extent and nature of organic coverage of soil mineral surfaces assessed by a gas sorption approach. Geoderma. 149, 152-160.

Wagai, R., Mayer, L.M., Kitayama, K., Shirato, Y., 2013. Association of organic matter with iron and aluminium across a range of soils determined via selective dissolution techniques coupled with dissolved nitrogen analysis. Biogeochemistry. 112, 95-109.

Wiseman, C.L.S., Püttmann, W., 2005. Soil organic carbon and its sorptive preservation in central Germany, European Journal of Soil Science. 56, 65-76.

Wood, P.M., 1994. Pathways for production of Fenton's reagent by wood rotting fungi. FEMS Microbiology Reviews. 13, 313-320.

Zaidel'man, F.R., Nikiforova, A.S., Stepantsova, L.V., Safronov, S.B., Krasin, V.N., 2009. Manganese, iron, and phosphorus in nodules of chernozem-like soils on the northern Tamov Plain and their importance for the diagnostics of gley intensity. Eurasian Soil Science. 42, 477-487.

Zerva, A., Ball, T., Smith, K.A., Mencuccini, M., 2005. Soil carbon dynamics in a Sitka spruce (Picea sitchensis (Bong.) Carr.) chronosequence on a peaty gley. Forest Ecology and Management. 205, 227-240.

Zerva, A., Mencuccuni, M., 2005. Short-term effects of clearfelling on soil CO2, CH4, and N2O fluxes in a Sitka spruce plantation. Soil Biology and Biochemistry. 37, 2025-2036.

Table 1: Typical soil profile descriptions of Harwood Forest Gleysol, Stagnosol and Cambisol soils. Descriptions follow Hodgson (1976) with the exception of redoximorphic features that follow Schoeneberger et al (2002).

Gleysol	Stagnosol	Cambisol
0-10 cm Ao: Dark brown (7.5YR 3/2) stone-free humic silt, highly humified and non-fibrous with a weakly developed medium blocky structure. Contains few fine roots and rare medium roots, lower horizon boundary is straight, moderately clear and abrupt.	0-9 cm Ao: Blackish grey (7.5YR3/1), stone-free slightly sandy humified organic silt, with a weakly developed granular structure; contains common fine roots, and, lower horizon boundary distinct, abrupt and wavy.	0-3 cm Ah: Dark brown (7.5YR 3/2), stone-free sandy silt with a fine granular structure and abundant fine roots, lower horizon boundary wavy, sharp and moderately distinct.
10-20 cm A: Dark greyish brown (7.5YR 5/2) sandy clay loam with a moderately developed medium blocky structure. Contains few fine and rarer medium roots, few stones up to 3cm in length, and few distinct orange masses (7.5YR 5/4, 7.5YR 5/5). Lower horizon boundary is straight, clear and gradual.	9-20 cm A(g): Mottled grey brown (7.5YR 5/1.5), mineral and organo-mineral sandy clay loam with a moderately well-developed medium / fine blocky structure; contain few fine roots, occasional stones up to 30 cm long, and many distinct masses, nodules and hypocoatings around roots, stones and voids (7.5YR 4/6, 7.5YR 5/6, 7.5YR 3/4). Lower horizon boundary is sharp, distinct and straight.	3-12 cm A: Brown (7.5YR 4/4), sandy clay loam with a well-developed granular and fine blocky structure; contains rare stones 1-2cm in length, common fine roots, and few earthworm channels. Lower horizon boundary is straight, clear and gradual.
20-35+ cm Bg: Brownish grey (7.5YR 6/2)mineral, silty clay loam with a moderately developed medium blocky structure; contains rare medium and fine roots, frequent stone up to 7cm in length, and many distinct orange masses and few nodules and hypocoatings (7.5YR 4/4, 7.5YR 5/4, 7.5YR 4/5) associated with stone and ped surfaces.	20-45+ cm Bg: Grey (5BG 6.5/1) mineral sandy loam with a weakly developed coarse blocky structure; contains rare medium and fine roots, abundant stones up to 30 cm long, and many distinct masses and nodules (7.5YR5/8, 7.5YR5/4, 7.5YR 5/6, 7.5YR 4/4, 7.5YR 2.5/1).	12-32+ cm B(g): Greyish brown (7.5YR 4.5/2) sandy clay loam with a well-developed medium block structure; contains few medium faint masses and few fine distinct nodules (7.5YR 4/3, 7.5YR4/4, 7.5YR5/4) that increase in frequency with depth, few fine roots, and rare stones up to 5cm in length.

Table 2: Summary of preliminary investigations into evidence of edge effects and resin interactions affecting moderately and strongly impregnated Fe nodules.

		C (wt %)		O/C		Fe (wt %)		Fe/C		Al (wt %)		Al/C	
Location		int	ed	int	ed	int	ed	int	ed	int	ed	int	ed
Treatment	None	35.7	46.3	1.75	1.05	16.0	8.9	0.80	0.37	2.1	2.5	0.13	0.07
	Oxalate	37.8	45.7	1.60	1.09	16.5	10.1	0.83	0.45	2.4	2.7	0.12	0.08
	Dithionite	45.5	49.8	1.12	0.79	0.3	0.3	0.01	0.01	4.0	3.5	0.14	0.08
F Statistic	Location	3.60		6.44*		7.1*		4.82*		0.01		2.77	
	Treatment	1.38		2.34		30.93*		13.43*		4.19*		0.09	
	Interaction	0.23		0.32		2.26		1.48		0.41		0.06	

int - internal (> 50 μm from feature edge), ed - edge (< 50 μm from feature edge), data analysed using GLM ANOVA, * indicates $p < 0.05$, wt % and elemental ratios are arithmetic means; 15 Fe nodules were analysed, with 3 - 6 point analyses in both the 'internal' and 'edge' zones.

Table 3: Bulk soil chemical characterisation based on the mean of five replicate soil profiles (only one profile for the Cambisol) and three replicate sub-samples for each profile (figures in brackets show one standard deviation).

Soil type and depth (cm)	pH	LOI SOM content (%)[1]	Particle Size Distribution (%)			Total soil concentration (mg g^{-1})		Oxalate[6]: Dithionite[7]		SOC content associated with Fe oxides (mg g^{-1})[2]
			60-2000 µm	2-60 µm	< 2 µm	Fe	Al	Fe	Al	
Gleysol										
0-10	4.1 (.7)[3]	24 (15)[3]	51[3]	46[3]	3[3]	13 (4)[3]	14(8)[3]	0.48 (.17)[3]	0.66(.18)[3]	53.18 (27.51)[3]
10-20	4.5 (1.1)	6.6 (2.0)	53[3]	44[3]	3[3]	17 (7)	19(4)	0.11 (.13)	0.56(.25)	28.28 (8.83)
20-30	4.3 (.5)	4.4 (1.6)	41[3]	52[3]	7[3]	23 (4)	25(11)	0.11 (.07)	0.98(.18)	14.98 (8.19)
Stagnosol										
0-10	3.9 (.1)[4]	24 (6)[4]	54[3]	44[3]	2[3]	12 (6)[4]	15(3)[4]	0.23 (.08)[4]	0.50(.35)[4]	44.63 (14.14)[4]
10-20	4.3 (.4)	9.2 (3.3)	55[3]	42[3]	3[3]	10 (3)	18(5)	0.23 (.09)	1.02(.40)	22.10 (8.43)
20-30	4.7 (.8)	5.3 (1.1)	28[3]	67[3]	5[3]	11 (4)	11(4)	0.12 (.06)	0.77(.29)	12.58 (3.36)
Cambisol										
0-10	5.4[5]	8.5[5]	53[3]	45[3]	2[3]	13[5]	16[5]	0.11[5]	0.44[5]	4.72[5]
10-20	5.3 (.1)	6.8 (.1)	64[3]	34[3]	2[3]	13 (1)	14 (2)	0.09 (.02)	0.45(.05)	17.37 (4.06)
20-30	5.1 (.0)	5.4 (.3)	72[3]	27[3]	1[3]	13 (2)	11 (4)	0.09 (.09)	0.58(.22)	14.55 (2.03)

[1]LOI SOM (16 hours, 450°C), [2]SOC determined by Elemental Analyser, [3]values determined as mean of single soil samples from five replicate profiles, [4]values determined as means of single soil samples from two replicate profiles and [5]values determined for single soil samples from one profile, [6]0.02 M sodium oxalate (NaOx) extraction method, [7]dithionite citrate bicarbonate (DCB) extraction sequentially after oxalate extraction.

Table 4: Mean frequencies of void, mineral, SOM and Fe pedofeatures in Gleysol, Stagnosol and Cambisol soils as determined by point counting in PPL of thin sections using magnification of x 100 (figures in brackets show one standard deviation).

Micromorphological feature	Cambisol	Stagnosol			Gleysol		
	5-15 cm A[3]	5-10 cm Ao[****]	5-15 cm A(g)[1]	20-30 cm Bg[2]	5-10 cm Ao[****]	5-15 cm A[1]	20-30 cm Bg[2]
Void space	26.4	25.9 (7.1)[a]	14.7 (5.6)[a]	17.4 (2.2)[a]	20.8 (10.6)[a]	16.2 (3.5)[a]	17.7 (9.3)[a]
Mineral grain	33.8	12.8 (14.01)[b]	27.7 (2.6)[a]	29.6 (1.8)[a]	11.2 (7.7)[b]	20.0 (5.3)[a]	18.0 (5.4)[ab]
Organ residue	.6	.1 (.2)[ab]	.1 (.1)[a]	.0 (.0)[ab]	.0 (.0)[b]	.0 (.0)[b]	.0 (.1)[a]
Tissue residue	2.2	6.0 (3.5)[a]	.5 (.6)[b]	.5 (.4)[b]	.0 (.0)[b]	.0 (.0)[b]	.0 (.1)[b]
Cellular residue	2.1	6.7 (4.7)[a]	.9 (.6)[b]	.2 (.0)[b]	.2 (.2)[b]	.0 (.1)[b]	.2 (.1)[b]
Amorphous organic fine material	34.1	48.3 (19.7)[ab]	54.7 (5.0)[ab]	52.1 (5.5)[ab]	67.4 (5.3)[a]	63.7 (4.5)[a]	44.1 (20.1)[b]
Weakly impregnated orthic Fe nodules	12.4	13.9 (19.5)[b]	17.8 (11.8)[b]	9.4 (1.7)[b]	38.5 (16.6)[ab]	48.4 (6.7)[a]	24.0 (10.1)[ab]
Moderately impregnated orthic Fe nodules	10.8	16.3 (13.3)[ab]	3.0 (1.9)[b]	3.1 (1.4)[ab]	20.8 (14.1)[a]	7.9 (3.7)[ab]	9.5 (4.6)[ab]
Strongly impregnated orthic Fe nodules	.4	3.4 (4.8)[a]	1.7 (1.8)[a]	2.7 (1.3)[a]	3.0 (3.0)[a]	1.3 (1.2)[a]	1.7 (1.0)[a]
Strongly impregnated anorthic or disorthic Fe nodules	6.1	1.4 (.45)[a]	.7 (.1)[a]	2.0 (.28)[a]	1.9 (.0)[a]	2.2 (.2)[a]	2.7 (.1)[a]

[1]Based on mean values from three slides from each of five soil profiles; [2]Based on mean values from one slide from each of five soil profiles; [3]Based on mean of two slides from one soil profile. For each soil property, values that do not share a common letter have significantly different frequencies at the 95% confidence interval (Tukey pairwise comparisons).

Table 5: Summary table of significant (p <0.05) Chi Square relationships between the presence of organic matter and the presence of Fe pedofeatures based on the point-count data.

Soil, Depth and Horizon	Significant relationships (χ square p<0.05)		
	Organic Matter feature	**Fe pedofeature**	**Sign of Correlation**
Stagnosol 5-15cm A(g)	Cell and Tissue residues	Weakly and Strongly impregnated orthic nodules	+
	Amorphous organic fine material	Weakly and Strongly impregnated orthic nodules	+
Stagnosol 20-30cm Bg	Cell and Tissue residues	Weakly and Strongly impregnated orthic nodules	+
	Amorphous organic fine material	Strongly impregnated anorthic / disorthic nodules	+
Gleysol 5-15cm A	Cell and Tissue residues	Weakly and Strongly impregnated orthic nodules	+
	Amorphous organic fine material	All classes of Fe pedofeatures	+
Gleysol 20-30cm B(g)	Cell and Tissue residues	Weakly and Strongly impregnated orthic nodules	+
	Amorphous organic fine material	All classes of Fe pedofeatures	+
Cambisol 5-15cm A	Organ residues	Weakly impregnated orthic nodules	+
	Amorphous organic fine material	Weakly and Strongly impregnated orthic nodules	+

Table 6: Mean C, Fe and Al concentrations of soil features at each stage of the sequential dissolution procedure from the A (5-15 cm) and B (20-30 cm) horizons of the Harwood Forest soils.

Feature	Before						After oxalate						After dithionite					
	% C	% Fe	% Al	Fe/C	Fe+Al /C	O/C	% C	% Fe	%Al	Fe/C	Fe+Al /C	O/C	% C	% Fe	%Al	Fe/C	Fe+Al /C	O/C
Resin	78[bc]	.32[c]	.28	.00	.01	.24[bc]	72[ac]	.58[c]	.34	.01	.01	.37[a]	69[ab]	.09[ab]	.28	.00	.01	.39[a]
Cambisol Groundmass A horizon (5-15cm)	65	1.42[c]	1.68	.02[c]	.05	.38[c]	62	1.07[c]	1.71	.02	.05	.49	62	.23[ab]	1.56	.00[a]	.03	.49[a]
Gley Groundmass A horizon (5-15cm)	56	.74[bc]	3.72	.01[bc]	.09[c]	.58	54	.30[a]	3.10	.01[ac]	.07	.65	57	.15[a]	2.51	.00[ab]	.05[a]	.57
Gley Groundmass B horizon (20-30cm)	36	3.06	4.88	.09[c]	.23	1.15	33	2.68	4.75	.08	.24	1.52	39	1.41	4.23	.03[a]	.15	1.15
Organ and tissue residue	68	1.98[bc]	.75[bc]	.03[bc]	.04[bc]	.39	70	.21[a]	.16[a]	.00[a]	.01[a]	.40	69	.03[a]	.16[a]	.00[a]	.00[a]	.40
Black amorphous fine organic material	71	.88[bc]	.87[bc]	.01[bc]	.02	.35	73	.28[ac]	.33[a]	.00[ac]	.01	.35	71	.04[ab]	.17[a]	.00[ab]	.01	.35
Moderately impregnated orthic Fe pan	59[b]	4.92[bc]	.56[bc]	.08[bc]	.09[b]	.44[b]	53[a]	9.07[ac]	1.17[ac]	1.71[ac]	.19[ac]	.60[a]	57	.22[ab]	2.08[ab]	.00[ab]	.04[b]	.54
Weak to moderate orthic groundmass Fe impregnation	47[bc]	6.92[bc]	3.32	.18[bc]	.26[bc]	.81	53[a]	2.51[ac]	2.68	.05[a]	.11[a]	.66	53[a]	.23[ab]	3.28	.01[a]	.10[a]	.71
Weak to moderate orthic tissue Fe impregnation	57	9.03[bc]	.96	.35[c]	.38[c]	.71	60	5.01[ac]	1.37	.11	.13	.54	63	.10[ab]	.97	.00[a]	.02[a]	.50
Strong anorthic/ disorthic Fe nodules	22[c]	27.59[bc]	2.67	1.93[bc]	2.09[bc]	2.59[bc]	29[c]	22.67[ac]	2.40	1.28[ac]	1.41[ac]	2.03[ac]	48[a]	.59[ab]	3.29	.02[ab]	.12[ab]	.94[ab]

Superscript letters denote significant differences (p<0.05) using Tukeys HSD, (a) denotes this variable differs significantly from the pre-extraction 'Before' state, (b) from the 'After oxalate' state, and (c) from the 'After dithionite' state
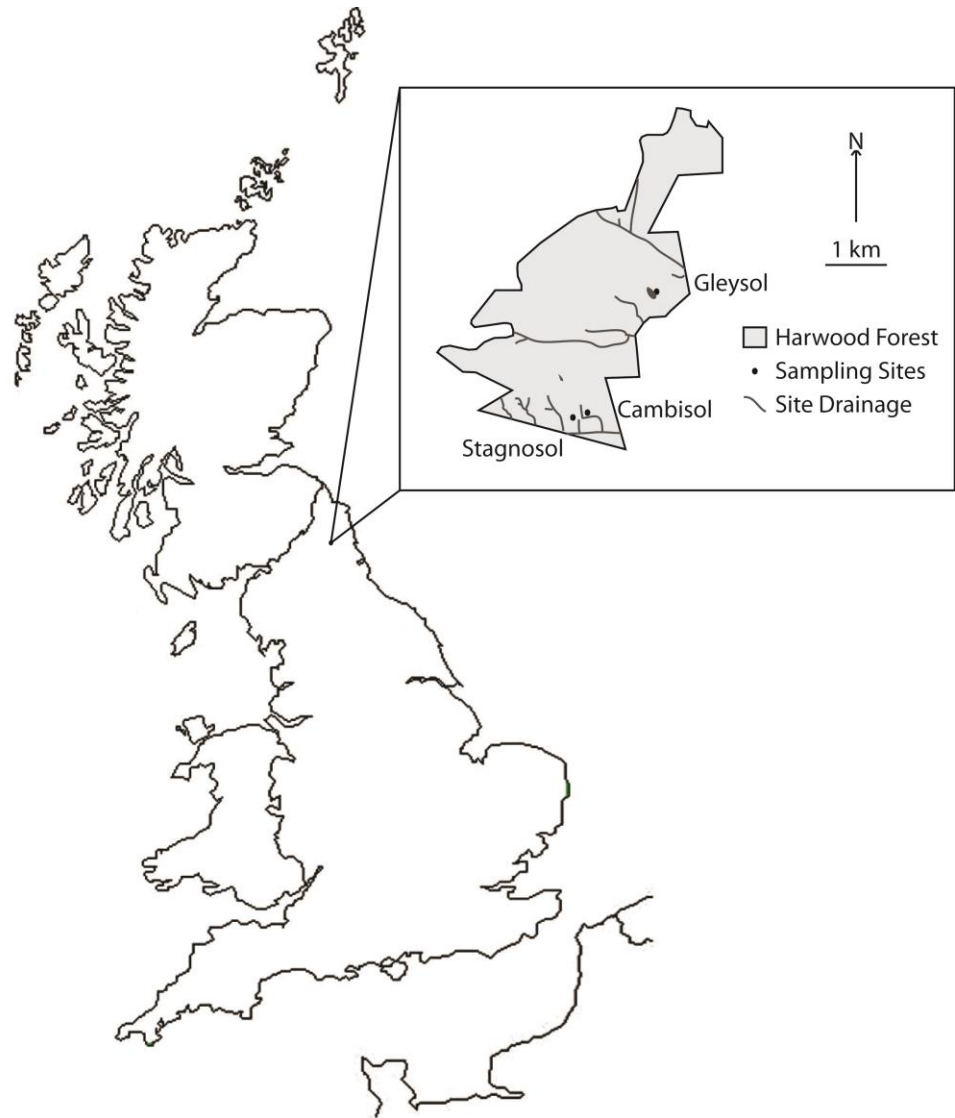
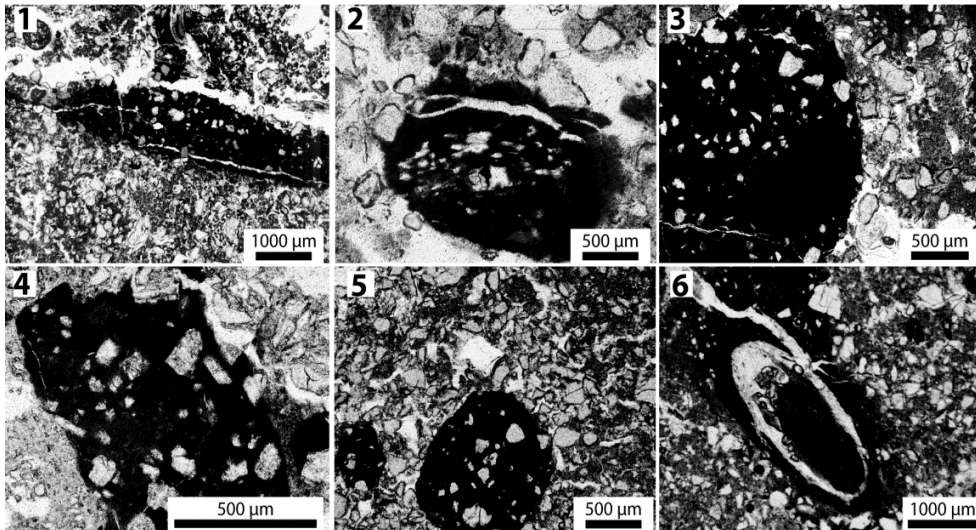Figure 1: Location map of the Harwood Forest, Northumberland, UK study site.

Figure 2: Typical examples of SOM and Fe pedofeatures seen under plane polarised light in thin section. 1- fragment of iron pan in PPL, 2 - degraded organic matter moderately impregnated with Fe, 3 - strongly impregnated anorthic Fe nodule, 4- moderately impregnated orthic Fe nodule, 5- strongly impregnated disorthic Fe nodule, 6 - partially degraded root tissue impregnated with Fe.
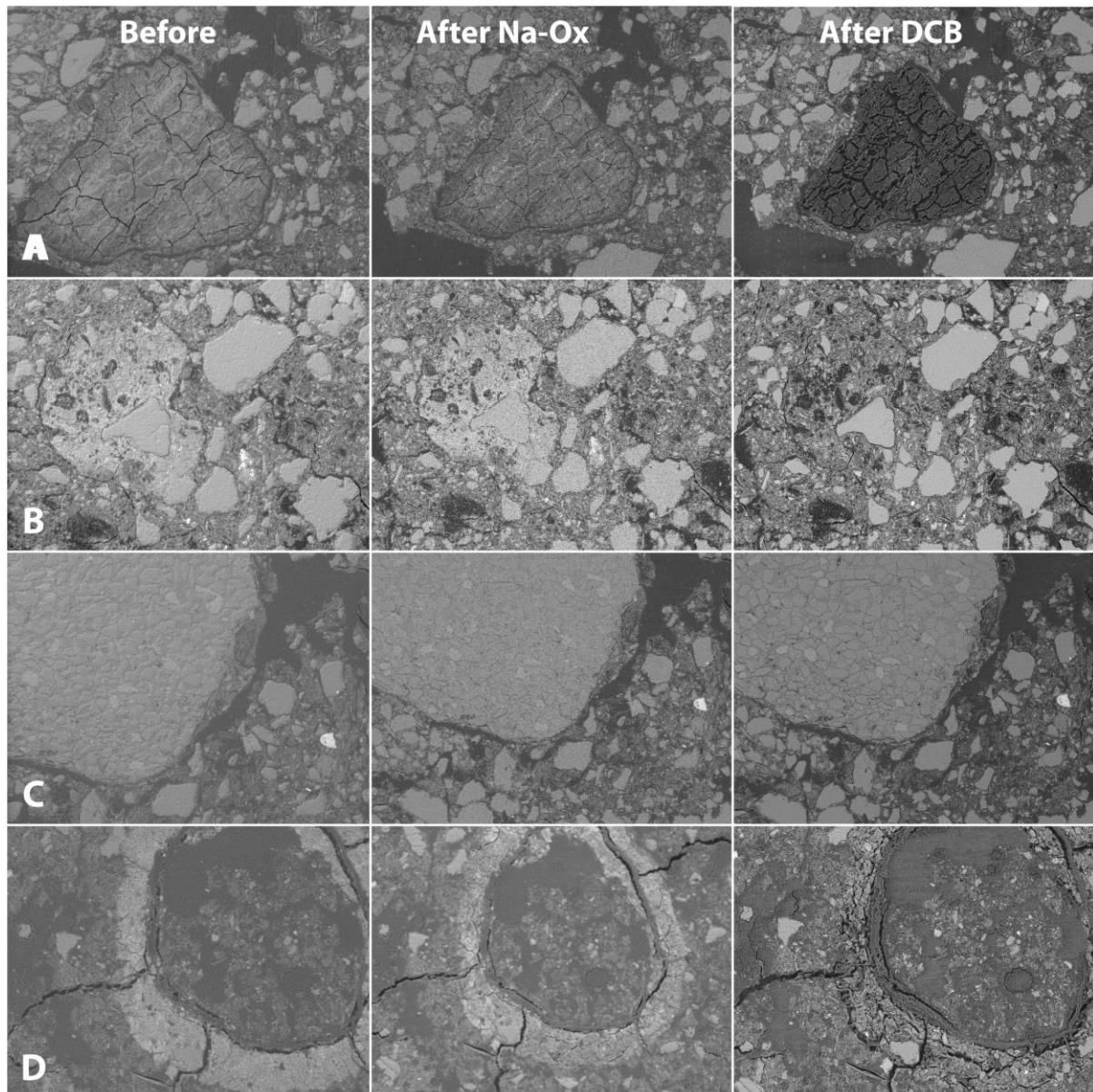
Figure 3: Back Scattered Electron images of soil features before and following selective dissolution in 0.02 M sodium oxalate (Na-Ox) and dithionite-citrate-bicarbonate (DCB): A, anorthic black nodule showing loss of Fe following DCB extraction revealing a core of organic matter, Gleysol, 20-30 cm, B, orthic strongly impregnated Fe nodule showing loss of Fe following DCB extraction revealing soil groundmass, Stagnosol, 5-15 cm, C, rock fragment showing little change after both extractions, Stagnosol, 20-30 cm, D, root tissue impregnation showing partial loss of Fe after Na-Ox and complete loss after DCB extractions, Gleysol, 5-15 cm.